LA-UR-13-20426
Approved for public release; distribution is unlimited.

Title: Recent Magneto-Inertial Fusion Experiments on FRCHX

Author(s): Degnan, J. H.; Amdahl, D. J.; Domonkos, M.; Grabowski, C.; Ruden, E. L.; White, W. M.; Wurden, Glen A.; Intrator, Thomas P.; Sears, Jason A.; Weber, Thomas; Waganaar, W. J.; Frese, M. H.; Frese, S. D.; Camacho, J. F.; Coffey, S. K.; Makhin, V.; Roderick, N. F.; Gale, D. G.; Kostora, M.; Sommars, W.; Bauer, B.; Fuelling, S. R.; Lynn, A. G.

Intended for: 24th IAEA Fusion Energy Conference 2012, 2012-10-08/2012-10-13 (San Diego, California, United States)

Recent Magneto - Inertial Fusion Experiments on FRCHX

J. H. Degnan[1], D. J. Amdahl[1], M. Domonkos[1], C. Grabowski[1], E. L. Ruden[1], W. M. White[1], G. A. Wurden[2], T. P. Intrator[2], J. Sears[2], T. Weber[2], W. J. Waganaar[2], M. H. Frese[3], S. D. Frese[3], J. F. Camacho[3], S. K. Coffey[3], V. Makhin[3], N. F. Roderick[3], D. G. Gale[4], M. Kostora[4], W. Sommars[4], B. Bauer[5], S. R. Fuelling[5], A. G. Lynn[6]

[1] Air Force Research Laboratory, Directed Energy Directorate, Kirtland Air Force Base, New Mexico, USA 87117
[2] Los Alamos National Laboratory, MS-E526, Los Alamos, New Mexico, USA 87545
[3] NumerEx, LLC, Albuquerque, New Mexico, USA 87106
[4] SAIC, Albuquerque, New Mexico USA 81313
[5] University of Nevada, Reno, Nevada, USA 89557
[6] University of New Mexico, Albuquerque, NM 87131

E-mail contact of main author: AFRL/RDHPWorkflowOrgMailbox@kirtland.af.mil

Abstract. Magneto-Inertial Fusion (MIF) approaches take advantage of embedded magnetic field to improve plasma energy confinement by reducing thermal conduction relative to conventional inertial confinement fusion (ICF). MIF reduces required precision in the implosion and the convergence ratio. Since 2008 [1], AFRL and LANL have developed one version of MIF. We have (1) reliably formed, translated, and captured Field Reversed Configurations (FRCs) in magnetic mirrors inside metal shells or liners in preparation for subsequent compression by liner implosion; (2) imploded a liner with interior magnetic mirror field, obtaining evidence for compression 1.36 T field to 540 T; (3) performed a full system experiment of FRC formation, translation, capture, and imploding liner compression operation; (4) identified by comparison of 2D-MHD simulation and experiments factors limiting the closed- field lifetime of FRCs to about half that required for good liner compression of FRCs to multi-keV, 10^{19} ion/cm^3, high energy density plasma (HEDP) conditions; and (5) designed and prepared hardware to increase that closed field FRC lifetime to the required amount. Those lifetime experiments are now underway, with the goal of at least doubling closed-field FRC lifetimes and performing FRC implosions to HEDP conditions this year. These experiments have obtained imaging evidence of FRC rotation, and of initial rotation control measures slowing and stopping such rotation.

1. Introduction

In Magneto-Inertial Fusion (MF), one uses magnetic inhibition of electron thermal conduction to greatly reduce the required implosion velocity and density – radius product relative to un-magnetized inertial fusion concepts [2]. We report here on progress in developing the version of MIF that uses a Field Reversed Configuration (FRC), formed by a reversed field theta discharge, and its subsequent compression by an imploding metal shell or liner, which is driven by a Z-pinch geometry discharge [2,3]. We previously reported on the successful demonstrations of imploding aluminum liners with size, radial convergence, uniformity, and implosion velocity suitable for compressing an FRC [4], and on the use of deformable liner – electrode contacts, which enable the use of large electrode apertures, suitable for FRC injection [5,6]. Our colleagues from Los Alamos and we have reported on formation of FRC's at the Los Alamos FRX-L facility, which have density ~ 5 x10^{16} cm^{-3}, ion + electron temperature ~ 400 eV, flux exclusion radius ~ 2 cm, and lifetimes ~ 10 μs [3,7]. We have reported on the essential reproduction of such a facility and its experimental results adjacent to the AFRL Shiva Star capacitor bank, which is used to drive liner implosions [8]. We have also previously reported 2D-MHD simulations of FRC formation, translation to liner interior, and FRC compression to multi-KeV temperatures [5,6]. More recent progress includes performing liner implosions with magnetic mirror fields interior to the liner; an engineering test of the full system including mirror fields, FRC formation translation, and capture, with liner implosion operation; an experimental series to improve captured FRC lifetime by improving flux capture using RF assisted pre-ionization, optimizing the relative timing of the several capacitor discharges to form the FRCs, and by introducing rotation control using biased rings and gas puffing to enable the biased ring operation. Recent progress also includes improved 2D-MHD simulation fidelity to experiments on FRC formation and diagnostic capture magnetic probe and interferometry signatures. Prior reports by a number of researchers suggest the general concept of using liners to compress plasmas and research on shorter or lower velocity liners [9-22], and implosion of a Cu-W liner with explosives to compress flux to 200 T [23].

2. Experiment Description

The experiment hardware is shown in Fig. 1. The FRC is formed using a reversed field theta discharge, employing 6 capacitor bank discharges to form, guide, and trap the FRC. The FRC formation begins with a 130 μs rise discharge establishing a ~ 0.4 T axial bias field. Cusp fields with 40 μs rise enhance magnetic field reconnection.

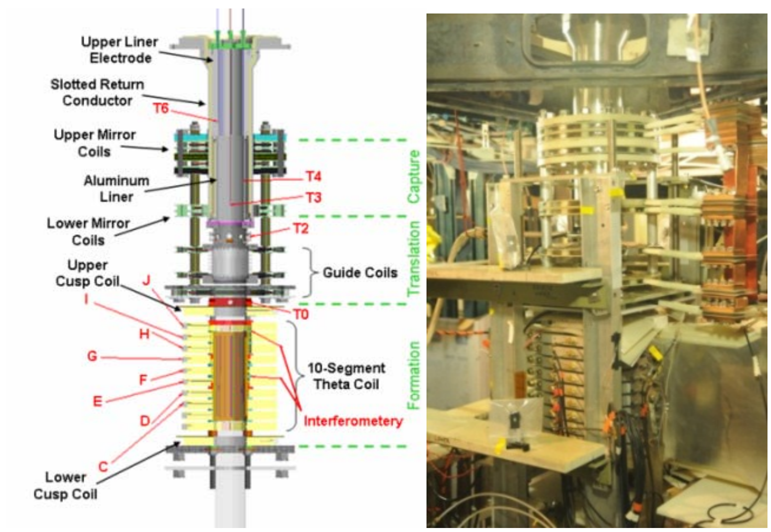

FIG. 1: Illustration and photo of FRC formation – capture - compression load.

The FRC is formed in a 50 to 100 milliTorr deuterium gas prefill inside a 10 cm diameter quartz tube inside the segmented theta coil. The coil is segmented for diagnostic access. The gas is pre-ionized using a 1 μs ringing theta pinch geometry discharge. Ideally, the plasma formed at this point would be fully diffused in the axial bias field. Then a 3.2 to 3.3 μs rise, ~ 1.5 to 2 T reverse bias axial field is applied to complete FRC formation. The theta coils feature a conical bore to propel the FRC into the guide and mirror regions of the apparatus. The guide and mirror coils are energized by a relatively slow 4.7 ms rise capacitor bank. The guide and mirror field inside the Al liner is formed by an array of coils downstream of (above) the formation region, with the mirror field inside the Al liner. This field is diffused through the liner implosion hardware and related structure. An example of the axial profile of this predominantly axial guide and mirror fields is shown in Fig. 2, with bias and cusp field contributions also shown. Large area inductive magnetic probe measurements and 3D magnetic diffusion calculations using COMSOL agree substantially on this field profile. This field is diffused through the liner implosion hardware and related structure. The 30 cm long x 10 cm diameter x 0.11 cm thick liner implosion is driven by a 4.5 MJ, 12 MA, 85 kV discharge produced by the AFRL Shiva Star capacitor bank.

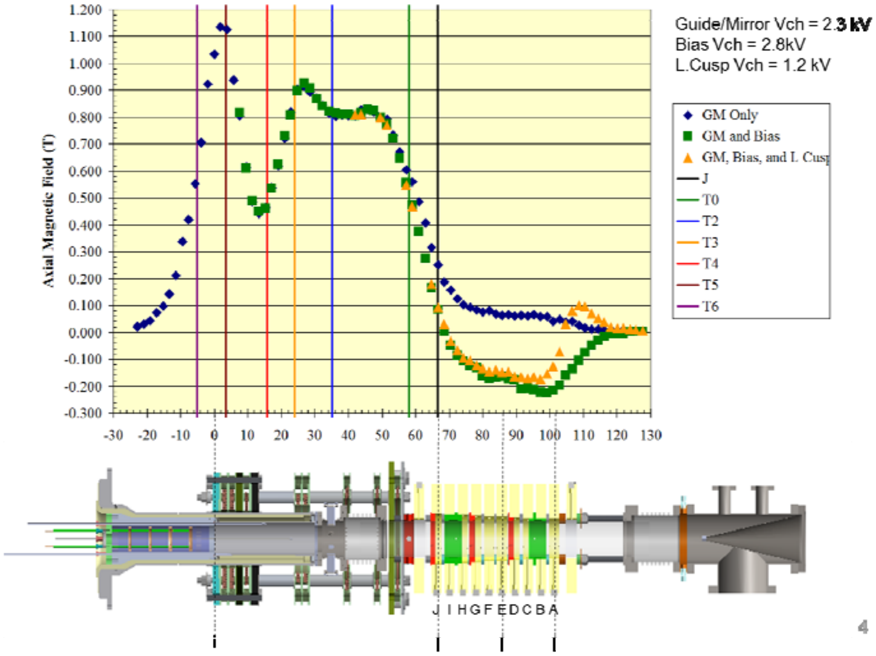

FIG.2 Axial guide and mirror field measured by large area probes at 6.1 ms after guide and mirror field discharge, with bias and cusp field contributions also shown.

Diagnostics include pulsed power current and voltage, magnetic probes, flux loops, fast multi-frame imaging, flash radiography, optical, Vacuum Ultra-Violet and X-ray diodes, optical spectroscopy, neutron activation, BTI bubble, and scintillator photomultiplier tube detectors.

3. Some experimental results

Liner implosion experiments with an operationally relevant interior magnetic mirror field obtained evidence for compression 1.36 T field to 540 T, by comparison liner inner and outer radius timing from flash radiography with MHD simulation, as illustrated in Fig.3.

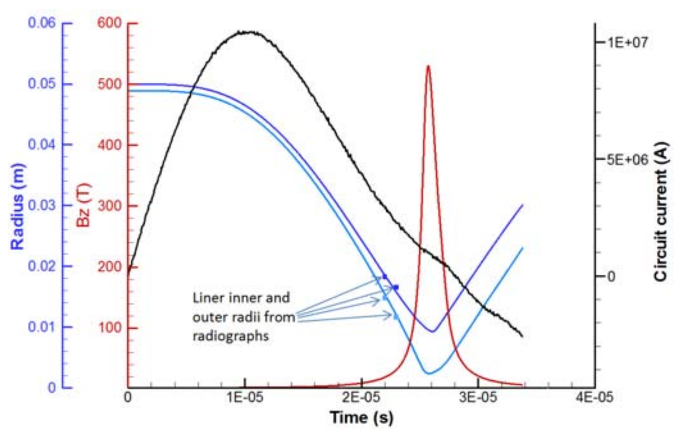

FIG.3 MHD calculations and radiography data for a liner-on-field compression experiment.

A full system engineering systems test which exercised the FRC formation discharges and liner implosion was successful in the pulsed power operations sense, but the signatures of plasma compression were weak, which was expected because captured FRC lifetimes were not yet what we believe are needed (about 20 μs, depending on relative timing of liner implosion discharge and FRC reversed field formation discharge). A subsequent experimental campaign, using internal magnetic probes in the liner-mirror region, has confirmed FRC capture, but with insufficient lifetime to support compression. We are now implementing measures to increase the lifetime. One approach uses a two-stage pre-ionization to enhance trapped bias flux. The first stage uses RF to enable better flexibility in the timing of the second stage pre-ionization and the reverse field discharge. This two-stage pre-ionization in which the RF electric fields are axial, achieved using a pair of ring electrodes outside the quartz tube above and below the formation region, appears to result better flux capture and larger FRC exclusion radius. These measures also include using charged rings above the liner/mirror region to control end shorting as a means to reduce or stop life-limiting FRC rotation. Use of the rings, requires replacing the approximately 50 milliTorr deuterium gas prefill with a gas puff, if one needs to use ring voltages above 200 volts.

An FRC, once formed, starts to rotate due, in part, to plasma conditions (lower temperature, higher density) at the vacuum chamber wall where the open magnetic field lines outside the separatrix exit the system. The Generalized Ohm's Law's ∇p_e term in the electric field implies that a non-rotating FRC will have an E field crossing the B field lines at the wall [24]. Whether the wall is dielectric or (especially) metal, the conductivity of the wall or plasma layer there will carry current and eventually short out this E field. This current and its associated B field introduce torque at the separatrix and cause unstable viscous sheared flow across the seperatrix, which leads to rotation of the FRC [25]. Supporting this E field with an external circuit coupled to conducting rings placed in the B-field exit region may slow or prevent rotation.

Some examples of magnetic field signals and exclusion radii in the capture region, in the magnetic mirror well inside the liner, obtained using both the RF first stage ionization and biased rings, are shown in Fig. 4. The excluded radius is obtained from the magnetic probe data using, for example, the Tuszewski method [26]. The maximum exclusion radius FWHM, a measure of lifetime in the trapped region, is in these examples 11.5 μs for 800 volt ring bias.

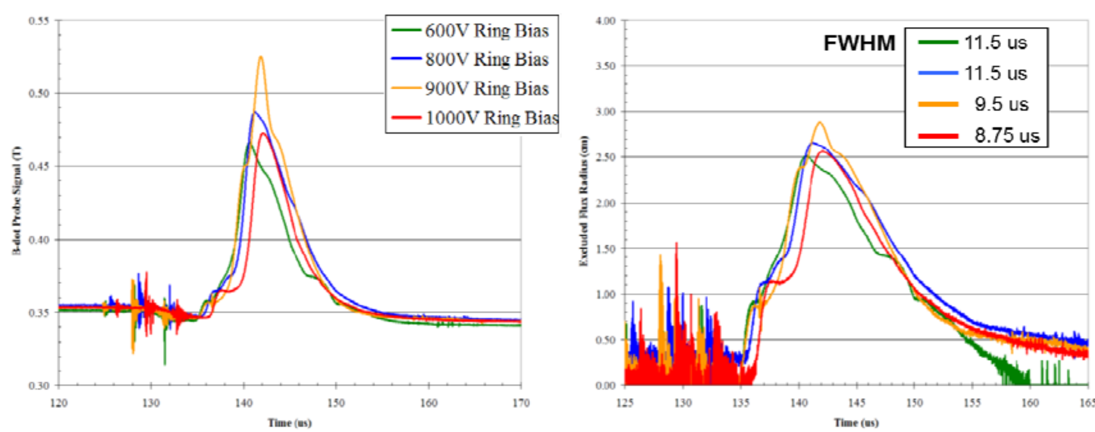

FIG. 4 Magnetic field signals (left) and exclusion radii (right) in the capture region, using RF first stage ionization and biased rings. Horizontal scales are time, 5 μs/div. Vertical scales are .05 Tesla/div and 0.5 cm/div.

The photos in Fig. 5 provide an example of observed plasma rotation both with (left) and without (right) a bias voltage applied to the rings. Lower inductance connections are needed for faster rotation control.

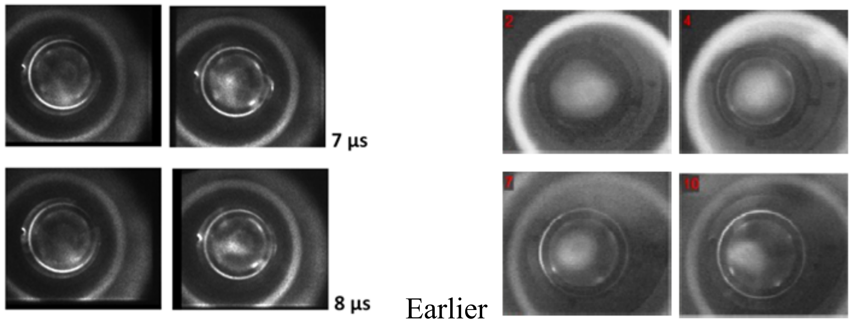

FIG.5 Axial view images showing rotation of decaying FRC with (later left) and without (later right) biased ring rotation control. Time is from start of first frame exposure. Four bright spots due to probes in capture region. Earlier frames for cases with more flux capture and higher bias ring voltage show intact, symmetric luminosity until 3 μs *after probe luminosity indicates entrance into trapping region*

Axial view vacuum ultraviolet images using a soft x-ray pinhole snout coupled to a fluorescer and observed by the multi-frame Hadland camera, confirm the hollow profiles expected of an FRC [27]. With time resolved visible spectroscopy (390-510 nm range), we observe clean (Stark-broadened) deuterium Balmer series lines, with trace Oxygen impurity, in the theta coil formation region. By the time the translating FRC reaches the capture region, we have evidence of plasma wall interactions, bringing in additional (metallic) impurities. This needs further study, including radial resolution, to see if central region remains low in impurity.

More recently, we have obtained improvements in this measure of trapped lifetime reaching these levels without the use of RF and bias rings, when increasing the firing delay between the fast theta discharge used for ionization and the main theta reversed field discharge. We are now combining this with RF first stage ionization and a faster response bias ring system.

4. Improved fidelity of simulations to experiment

Experiment design and interpretation of data have been strongly coupled to and guided by 2 and 3D-MHD and extended MHD simulations. The examples shown here are simulations of experiments with both fixed (static, unimploded) and imploding aluminum liners, performed using MACH2 [28].

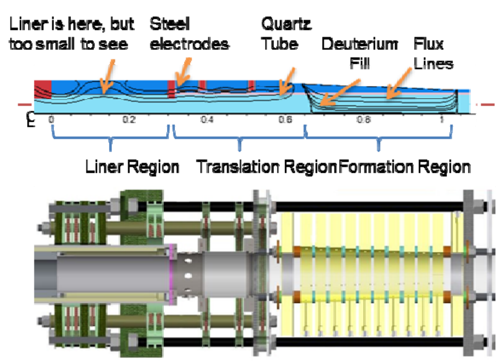

FIG.6 Simulation geometry compared to hardware.

These simulations include SESAME table EOS's and resistivities for materials, all three components of the magnetic fields, an energy-conserving model of the imploding deformable liner, flux-based field modeling of the time-dependent polodial fields, and use adaptive gridding for the FRC and a Lagrangian grid for the liner.

We have attempted to capture as much of the physical geometry as we can. AFRL's welldiagnosed static liner experiments are providing a lot of data we can use within our simulations and as a basis for validation of the simulation's representation of the experiment.

We have greatly improved our ability to model the FRCs that are being formed by using the 'time of first light' in the experimental data as an indicator of when the ionization and flux-trapping occurs, for our modeling of the pre-ionization. This technique produces capture region integrated B-dot signatures that are very much like those measured in the corresponding experiments.

The particular comparison shown in Fig.7 is based on an experiment performed in March of this year, using low level RF-induced pre-pre-ionization._Only part of the FRC was captured in the mirror fields in the static liner; some mass and flux escaped out the top (left hand side in picture). See Fig.8.

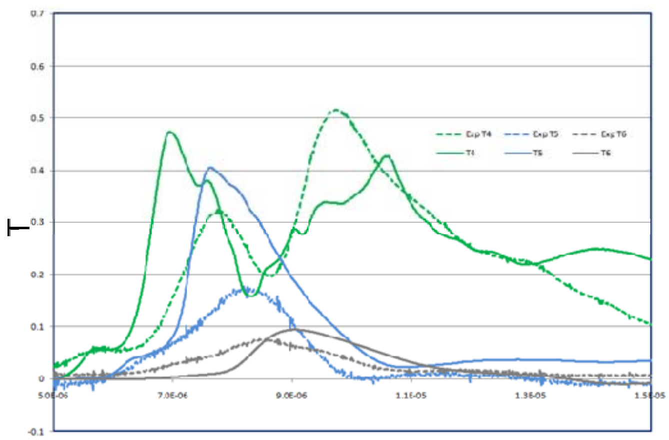

FIG.7 Simulation (solid) vs experiment (dashed) magnetic field at experiment probe locations in mid capture region (green, T4), exit mirror region (blue, T5) and beyond (downstream of, above) exit mirror (black, T6).

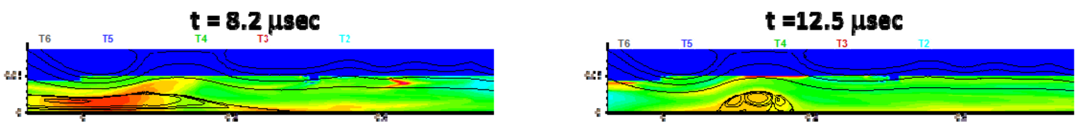

FIG.8 Simulation density contours for case shown in FIG 7. See FIG 6 for relation of geometry to hardware. The times are relative to the firing of the main theta reverse bias discharge.

The imploding liner experiments have an added complication of the timing of the main theta bank of the FRC relative to the main bank of the liner implosion. In order to maximize the lifetime of the FRC within the imploding liner, it is useful to have the liner accelerated and imploding when the FRC arrives, and the compression of the mirror fields by the liner must be accounted for. Here we have selected a 5.65 μs delay to put the low-RF FRC at the imploding liner ~ 12 μs into the implosion. The liner's inner radius is ~80% of its original 4.89 cm, and the mirror fields have decreased to 64% of nominal. Only a fraction of this FRC was captured. The simulation follows the compression of FRC by the liner – shown below with the liner radius at 5.06 mm. Notice that our 1 cm long FRC (16 μs) is now ~ 8 mm long..

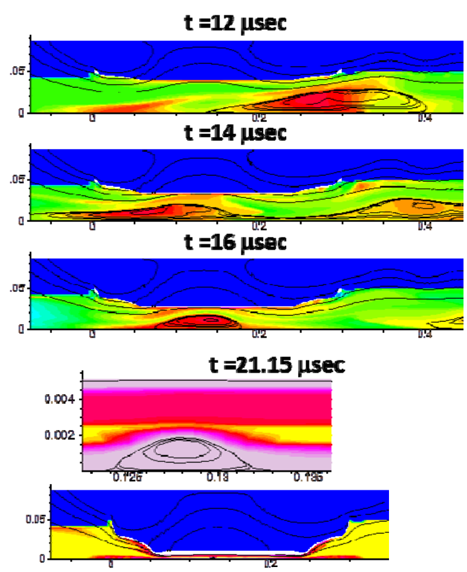

FIG.9 FRC approaches imploding liner, enters, splits, and portion is captured at 12 μs and subsequently compressed. Compressed density is ~10^{18}ions/cc. Peak initial captured density is ~ $3x10^{16}$ions/cc.

The simulations have also ta
and hence in the initial FRC affects the lifetime and the robustness of the FRC. We performed

a similar compression simulation with data from another March 2012 experiment with higher RF and higher bias field at the time of first light. This FRC has 67% more flux after its formation than the FRC we have been discussing. (1.257 mW vs 0.754 mW). We captured more of it, and the captured FRC Has more flux (0.415 mW vs 0.346 mW), is hotter (273 eV vs 209 eV), is less dense (N_i = 2.6E16 /cc vs 3.3E16 /cc), but slightly earlier capture time means less compression has occurred. This will improve its lifetime and its yield upon compression.

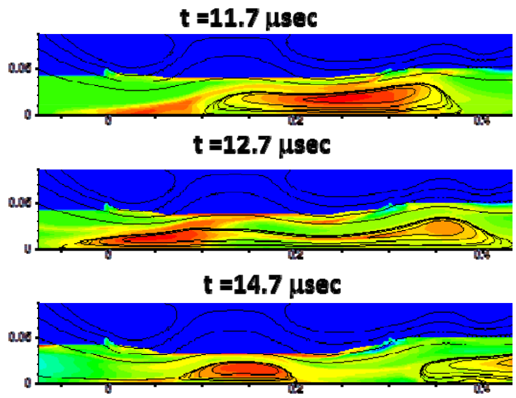

FIG.10 Simulation of experimental case with higher power RF pre-pre-ionization, and higher bias field at time of first light from ionization.

5. Future Work

An alternative to RF and bias rings which we may explore is to use a plasma gun for ionization and end shorting control. This has been employed, more than doubling the lifetime of lower energy density FRCs, as documented in the reports of Tri-Alpha Energy [29]. Future work will include FRC compression and study of FRC behavior and the liner inner surface during compression, which is in a warm dense matter state. These effects include, e.g., Rayleigh Taylor effects and liner material - plasma mixing under HEDP conditions.

6. References

[1] WURDEN,G.A, INTRATOR, T.P. et al, LA-UR-08-0796, "FRCHX Magnetized Target Fusion HEDLP Experiments", IC/P4-13, IAEA 2008 Fusion Energy Conference, Geneva, Switzerland, Oct. 13-18, 2008.

[2] SCHOENBERG, K.F., SIEMON, R.E. et al, “Magnetized Target Fusion, A Proof of Principle Research Proposal”, LA-UR-98-2413, 1998

[3] TACETTI, J. M. Taccetti et al, Rev. Sci. Instr. 74, 4314 (2003).

[4] DEGNAN, J.H. et al, “Implosion of Solid Liner for Compression of Field Reversed Configuration”, IEEE Transactions on Plasma Science 29, p.93-98 (2001).

[5] DEGNAN, J.H.et al, “Progress in Liner Implosions for Compression of FRC’s”, in Proceedings of the 2006 International Conference on Megagauss Magnetic Fields and Related Topics, p. 93, Ed. G. F. Kiuttu, R. E. Reinovsky, and P. J. Turchi, IEEE Catalog Number CFP06MEG-PRT, 2007.

[6] DEGNAN, J.H. et al, “Experimental and Computational Progress on Liner Implosions for Compression of FRC’s”, Transactions on Plasma Science 36, Part 1, p. 80, Feb 2008.

[7] ZHANG, S. Y. et al, “High density field reversed configuration plasma for magnetized target fusion”, IEEE Transactions on Plasma Science 34, no. 2, p. 223, April 2006.

[8] DEGNAN, J.H. et al, “Research on Field Reversed Configuration (FRC) formation and their compressio n using liners”, in Proceedings of Megagauss 12 Conference

[9] LINDEMUTH,I., KIRKPATRICK,R.,“Parameter space for magnetized fuel targets in Inertial Confinement Fusion”, Nucl. Fusion 23, 263 (1983)

[10] LINDEMUTH, I. et al., “Target plasma formation for Magnetic Compression/Magnetized Target Fusion”, Phys.Rev.Lett. 75, 1953 (1995)

[11] CHERNYSHEV, V.K., MOKHOV, V.N., “On the progress in the creation of powerful explosive magnetic energy sources for thermonuclear target implosion”, in Digest of Technical Papers: 8th IEEE International Pulsed Power Conference (IEEE, NY, NY, 1991), P.395-410

[12] FOWLER, C.M., “Intense Magnetic Fields” in Atomic Energy Research in the Life and Physical Sciences, 1960, (AEC Special Report, Jan. 1961), p.104.

[13] LINHART, J.G., KNOEPFEL, H., GOURLAN, C., “Amplification of magnetic fields and heating of plasma by a collapsing metallic shell”, Nucl.Fusion 1962 Supplement 2:733.

[14] WINSOR, N.K., BORIS, J.P., SHANY, R.A., “Plasma heating by flux compression”, Proceedings, Symposium on Plasma Heating and Injection, Varenna, Italy (Editorice Compositori, Bologna, 1973), p.227-231.

[15] VELIKHOV, E.P. et al, “Generation of megagauss magnetic fields using a liner compressed by high pressure gas”, Sov.Phys.-Tech.Phys.18, p.274 (1973).

[16] GOLOVIZNIN, V. et al, “Numerical simulation of dynamics of quasispherical metallic liner”, in “Megagauss Physics and Technology”, Second International Conference on Megagauss Magnetic Field Generation and related Topics, edited by P.J.Turchi (Plenum Press, New York, NY, 1980), p. 415

[17]TURCHI, P.J. et al, “Review of the NRL Liner Implosion Program”, *ibid*, p.395

[18] SHERWOOD, A.E. et al, “Results from the Los Alamos Fast Liner Experiment”, *ibid*, p. 391

[19] KAREEV, Ju.A. et al, “Liner thermonuclear system with superhigh magnetic field and $\beta>1$”, *ibid*, p. 399

[20] ANDRIANOV, A.M. et al, “Production of megagauss magnetic fields by compression of a magnetic field with a metallic liner”, *ibid*, p. 479

[21] MOKHOV, V. et al, “Possible solution of the controlled thermonuclear fusion problem based on magnetogasdynamic energy storage”, Sov.Phys. Dokl. 24, 557 (1979)

[22] CHERNYSHEV, V.K. et al, “Cylindrical liner: implosion dynamics under EMG magnetic pressure”, in Sixth International Conference on Megagauss Magnetic Field Generation and Related Topics, edited by M.Cowan and R.Spielman (Nova Science Publishers, Inc, Commack, NY, 1994), p.815

[23] ARMSTRONG, W.T., MORGAN, J.A., “Liner compression of magnetically confined FRC plasmas”, in "Megagauss Technology and Pulsed Power Applications", Fourth International Conference on Megagauss Magnetic Field Generation and related Topics, edited by C.M.Fowler, R.S.Caird, and D.J.Erickson (Plenum Press, New York, NY, 1987), p.683

[24] STEINHAUER, L.C., “End-Shorting and electric field in edge plasmas with application to field-reversed configurations,” *Phys. Plasmas* **9**, pp. 3851, 2002.

[25] RUDEN, E.L., “The FRC's n=2 rotational instability interpreted as the dominant Rayleigh-Taylor mode of a gyroviscous plasma with sheared toroidal flow,” *US-Japan exchange 2004: New directions and physics for compact toroids*, Santa Fe, NM, Sept. 14-16, 2004.

[26] TUSZEWSKI, M., Phys. Fluids 24, p. 2126, 1981; TUSZEWSKI, M., ARMSTRONG, W. T., Rev. Sci. Instr. 54, p. 1611, 1983

[27] WURDEN, G.A. and COFFEY, S.K., “A multi-frame soft X-ray pinhole imaging diagnostic for single-shot applications”, Rev. Sci. Instr. 83, 10E516 (2012)

[28] PETERKIN, Jr, R.E., FRESE, M.H., SOVINEC, C.R., “Transport of magnetic flux in an arbitrary co-ordinate ALE code”, J.Comp.Phys. 140, 148 (1998)

[29] GUO, H. Y.; BINDERBAUER, M. W., et al., "Formation of a long-lived hot field reversed configuration by dynamically merging two colliding high-β compact toroids", Physics of Plasmas, vol. 18, no.5, 56110 (2011).